Published in final edited form as:

Clin Cancer Res. 2019 September 15; 25(18): 5561–5571. doi:10.1158/1078-0432.CCR-19-0908.

Integrative molecular characterization of resistance to neoadjuvant chemoradiation in rectal cancer

Sophia C. Kamran[1,2], **Jochen K. Lennerz**[3], **Claire A. Margolis**[2,4], **David Liu**[2,4], **Brendan Reardon**[2,4], **Stephanie A. Wankowicz**[2,4], **Emily Van Seventer**[6], **Adam Tracy**[2], **Jennifer Y. Wo**[1], **Scott L. Carter**[2,5], **Henning Willers**[1], **Ryan B. Corcoran**[5], **Theodore S. Hong**[*,1], **Eliezer M. Van Allen**[*,2,4]

[1]Department of Radiation Oncology, Massachusetts General Hospital, Harvard Medical School, Boston, MA

[2]Broad Institute of MIT and Harvard, Cambridge, MA

[3]Department of Pathology, Center for Integrated Diagnostics, Massachusetts General Hospital, Boston, MA

[4]Department of Medical Oncology, Dana-Farber Cancer Institute, Harvard Medical School, Boston, MA

[5]Joint Center for Cancer Precision Medicine, Dana-Farber Cancer Institute/Brigham and Women's Hospital, Boston, MA

[6]Massachusetts General Hospital Cancer Center and Department of Medicine, Harvard Medical School, Boston, MA

Abstract

Purpose: Molecular properties associated with complete response or acquired resistance to concurrent chemotherapy and radiation therapy (CRT) are incompletely characterized.

Experimental Design: We performed integrated whole exome/transcriptome sequencing and immune infiltrate analysis on rectal adenocarcinoma tumors prior to neoadjuvant CRT (pre-CRT) and at time of resection (post-CRT) in 17 patients (8 complete/partial responders [R], 9 nonresponders [NR]).

Results: CRT was not associated with increased tumor mutational burden or neoantigen load and did not alter the distribution of established somatic tumor mutations in rectal cancer. Concurrent *KRAS*/*TP53* mutations (KP) associated with NR tumors and were enriched for an epithelial-mesenchymal transition transcriptional program. Furthermore, NR was associated with reduced CD4/CD8 T-cell infiltrates and a post-CRT M2 macrophage phenotype. Absent any local tumor recurrences, KP/NR status predicted worse progression-free survival, suggesting that local

Corresponding authors: Eliezer M. Van Allen, MD, Department of Medical Oncology, Dana-Farber Cancer Institute, Boston, MA 02215, USA, Phone: 617-632-2429, Fax: 617-632-2165, eliezerm_vanallen@dfci.harvard.edu, Theodore S. Hong, MD, Department of Radiation Oncology, Massachusetts General Hospital, Boston, MA 02114, USA, Phone: 617-726-6050, Fax: 617-726-8650, tshong1@mgh.harvard.edu.

*These authors contributed equally to this work.

immune escape during or after CRT with specific genomic features contributes to distant progression.

Conclusions: Overall, while CRT did not impact genomic profiles, CRT impacted the tumor immune microenvironment, particularly in resistant cases.

Keywords

biomarkers; whole exome sequencing; whole transcriptome sequencing; chemoradiation; tumor mutational burden

INTRODUCTION

Radiation therapy is used in the management of nearly two-thirds of cancers (1), often fulfilling the role of a curative treatment modality in place of surgery. Therapeutic radiation can be adapted to target tumors in various anatomical locations as well as various malignancies. The radiation dose and fractionation can be altered to maximize tumor-killing while sparing normal tissues (2). Radiation therapy is typically combined with concurrent chemotherapy (CRT) in locally advanced disease. When used neoadjuvantly, pathological downstaging is a surrogate of long-term outcome in many disease sites (3–7). For example, in rectal cancer (RC), approximately 9-20% of patients with locally advanced disease have a pathological complete response (pCR) to neoadjuvant CRT (8) while 20-40% of patients have little to no response (9,10). Predictive biomarkers of pCR remain to be established.

The major mechanism of radiation-induced cell killing is likely through DNA damage. There is, however, emerging evidence that radiation also has effects on the tumor microenvironment with variation based on anatomic site, tumor histology, and multiple other characteristics (11). These cell killing effects can be further augmented by combining radiation with radiosensitizing systemic agents (12). In addition, there is recent interest in the utility of radiation to alter the adaptive immune response to improve treatment outcomes by creating a local anti-tumor immune response that may be modulated into a systemic anti-tumor immune response with the use of immunomodulatory agents (13–15). Proposed mechanisms include possible creation of increased neoantigens or tumor mutational burden (TMB) through the DNA-damaging effects of radiation (16,17), the latter of which has been previously demonstrated to correlate with response after treatment with immune checkpoint inhibitors (18,19). Despite the widespread use of radiation therapy for solid tumors, there has been slow progress in predicting treatment outcomes to radiation to allow for personalization of therapy on an individual level (12,15). Biomarkers have been in use and ultimately transformed the field of systemic therapy while few predictive biomarkers are available for radiotherapy (12).

Using RC as our model (3,20), we hypothesized that a comprehensive assessment of patient-matched pre- and post-CRT specimens, examining both tumor-intrinsic and microenvironmental features from the tumor site, may reveal features associated with treatment response at the molecular level. To that end, we leveraged a cohort of locally advanced RC patients who underwent fluoropyrimidine-based CRT to a dose of 50.4 Gy followed by surgical resection and analyzed genomic tumor changes in the matched pre- and

post- treatment rectal tumor samples to identify drivers of resistance to neoadjuvant CRT and thereby identify biomarkers for patient stratification.

METHODS

Patient population and samples

We retrospectively identified patients with biopsy-proven locally advanced rectal cancer (defined as T3-4 or N+) who received neoadjuvant fluoropyrimidine-based chemotherapy concurrently with 50.4 Gy radiation therapy, followed by surgical resection within 8-11 weeks between 2010 and 2016 (20). Patients then went on to receive adjuvant systemic therapy, which consisted of FOLFOX (21). Patients had to have documented written consent through the institutional review board-approved protocol that collects tissue and whole blood specimens on patients with gastrointestinal malignancies in accordance with the Declaration of Helsinki and all applicable legal regulatory requirements. There were 77 patients who met initial criteria. Eligible patients had to have sufficient tumor tissue in study specimens of formalin-fixed, paraffin-embedded (FFPE) tissue sections from surgical samples, as well as a germline DNA specimen that was extracted from either peripheral mononuclear cells or histologically normal rectal tissue. Twenty patients were identified with sufficient tissue available. All patients were arbitrarily identified with no prior knowledge of genomic tumor status. All samples had to pass standard quality control measures. We identified 34 pre- and post-CRT matched tumor samples from 17 patients in our final cohort. Nine and 8 patients were classified as nonresponders (no evidence of any pathologic downstaging, NR) and responders (pathologic complete response or pathologic partial response, R) respectively at surgery based on pathologic evaluation.

DNA extraction and whole exome sequencing

DNA extraction, whole exome library prep and sequencing was performed for the samples as previously described (22,23). Slides were cut from FFPE blocks and examined by a board-certified pathologist to select high-density cancer blocks and ensure high purity of cancer DNA. Biopsy cores were taken from the corresponding tissue block for DNA extraction. DNA was extracted using Qiagen's QIAamp DNA FFPE Tissue Kit Quantitation Reagent (Invitrogen). DNA was stored at −20 °C.

Whole exome capture libraries were constructed from 100 ng of DNA from tumor and normal tissue after sample shearing, end repair, and phosphorylation and ligation to barcoded sequencing adaptors. Ligated DNA was size selected for lengths between 200 and 350 bp and subjected to exonic hybrid capture using The Broad Institute Genomics Platform Custom Illumina bait. The Illumina exome specifically targets approximately 37.7Mb of mainly exonic territory made up of all targets from the Agilent exome design (Agilent SureSelect All Exon V2), all coding regions of Gencode V11 genes, and all coding regions of RefSeq gene and KnownGene tracks from the UCSC genome browser (http://genome.ucsc.edu). The sample was multiplexed and sequenced using Illumina HiSeq technology.

Sequencing was performed to an average depth of 150 X. Data were analyzed using the Broad Picard Pipeline which includes de-multiplexing and data aggregation.

Quality control, variant calling

Initial data processing and analysis of exome sequence data were performed used Broad Institute pipelines and as previously described (23). Using the Broad Picard Pipeline for alignment, BAM files were uploaded into the Firehose infrastructure to manage intermediate analysis files executed by analysis pipelines. Quality-control modules in Firehose (24) were run to compare the tumor and normal genotypes and ensure concordance between samples. Of samples from 20 initial patients, 6 samples from three patients were abandoned because of high estimates of tumor contamination (25), inadequate coverage (<40x tumor average coverage), or low tumor purity (26). This yielded a final number of 17 total pairs of pre and post treatment tumors for analysis.

The MuTect algorithm (27) was applied to identify somatic single-nucleotide variants in targeted exons. Strelka (28) was used to identify small deletions or insertions, and alterations were annotated with Oncotator (29). Mutations were examined for distribution and type and confirmed using the integrative genomics viewer (30,31).

Transcriptome Capture Method cDNA Library Construction

Using established protocols (32), total RNA was assessed for quality using the Caliper LabChip GX2. The percentage of fragments with a size greater than 200nt (DV200) was calculated using software. An aliquot of 200ng of RNA was used as the input for first strand cDNA synthesis using Illumina's TruSeq RNA Access Library Prep Kit. Synthesis of the second strand of cDNA was followed by indexed adapter ligation. Subsequent PCR amplification enriched for adapted fragments. The amplified libraries were quantified using an automated PicoGreen assay.

200ng of each cDNA library, not including controls, were combined into 4-plex pools. Capture probes that target the exome were added and hybridized for recommended time. Following hybridization, streptavidin magnetic beads were used to capture the library-bound probes from the previous step. Two wash steps effectively remove any non-specifically bound products. These same hybridization, capture and wash steps are repeated to assure high specificity. A second round of amplification enriches the captured libraries. After enrichment the libraries were quantified with qPCR using the KAPA Library Quantification Kit for Illumina Sequencing Platforms and then pooled equimolarly. The entire process is in 96-well format and all pipetting is done by either Agilent Bravo or Hamilton Starlet.

Pooled libraries were normalized to 2nM and denatured using 0.1 N NaOH prior to sequencing. Flowcell cluster amplification and sequencing were performed according to the manufacturer's protocols using HiSeq 2500. Each run was a 76bp paired-end with an eight-base index barcode read. Data was analyzed using the Broad Picard Pipeline which includes de-multiplexing and data aggregation.

Neoantigen prediction

HLA-type was inferred using POLYSOLVER (33) which uses a normal tissue BAM file as input. It then employs a Bayesian classifier to determine the genotype for each patient. Neoantigens were predicted for each patient by defining all novel amino acid 9mers and 10mers resulting from mutations (23). We filtered out mutations with <3 supportive reads, or <30 total reads at the position. Neoantigen prediction continued based on whether predicted binding affinity to the patient's germline HLA alleles was <500 nM using NetMHCpan (34). Correlations and associated p values between neoantigen load and R versus NR was performed using Mann-Whitney U tests, p-values of <0.05 were considered significant.

Purity/ploidy, clonal/subclonal mutational calls

Purity and ploidy for each sample was estimated using ABSOLUTE algorithm (35). This algorithm integrates variant allele frequency distributions and copy number variants to estimate absolute tumor purity and ploidy and infer cancer cell fraction (CCF), which is the proportion of cancer cells in the sample which contain each mutation. An ABSOLUTE extension algorithm (35) was used to construct an inferred phylogenetic tree with clones, subclones, and evolutionary relationships in pre and post treatment tumor samples. As described in Brastianos et al (36), clones and subclones were determined through Markov Chain Montecarlo sampling using Dirichlet process Mixture Models on pre- and post-CRT mutation CCFs, which assigns mutations to subclones without pre-specifying the number of subclones. Mutations inferred to be in a subclone with a CCF ≥ 0.8 were described as "clonal" while those inferred to be in a subclone with CCF < 0.8 were called "subclonal." For each subclone, two CCFs were inferred; one CCF in the pre-treatment tumor and CCF in the post-treatment tumor (23).

Changes in mutational and neoantigen load

Changes in mutational, neoantigen, and indel load were calculated using a paired t-test of changes in paired samples with a null hypothesis of a difference of 0 (23). $p<0.05$ was considered to be statistically significant.

Discovery of resistance or sensitivity biomarkers

We used MutSig2CV (26) to identify significantly mutated genes across our cohort of pre-CRT and post-CRT tumors. Each altered gene in the pre-treatment tumors had a p-value calculated for mutational significance considering only mutations private to these samples. Similarly, a p-value of mutational significance considering only those mutations private to the post-treatment tumor was calculated. Adjustment for hypothesis testing was performed using a Benjamini-Hochberg FDR of 0.1 (23).

Gene expression profiling

Available RNA-Seq data were analyzed as previously described (37). Briefly, expression data were examined and adjusted for batch effects using ComBat (38) using the R Bioconductor package "sva" V3.8 (39). Gene set enrichment analysis (40) was run using https://genepattern.broadinstitute.org using 50 'Hallmark' gene sets to investigate differences in gene set expression in R vs. NR (pre-CRT R vs. pre-CRT NR; post-CRT R vs.

post-CRT NR) with 1000 permutations, type ‘gene_set.’ Gene level transcripts per million (TPM) were the input. Family-wise error rates were calculated to identify significant gene sets.

To determine the relationship between CRT and the immune landscape, we analyzed matched transcriptomes from the tumors using CIBERSORT (41) to deconvolute immune cell populations from bulk transcriptome data using immune-cell associated signatures. From this, we inferred overall immune infiltrate and relative immune cell populations in both the pre-CRT and post-CRT specimens. This was run using the CIBERSORT interface (https://cibersort.stanford.edu). The analysis was set to absolute quantification output. Input was gene level TPM and leukocyte gene signature matrix (LM22) (41) was used to deconvolve 22 immune cell subset populations. Absolute quantification normalizing by the 50th percentile of overall gene expression generated a metric that is comparable between samples. Correlations and associated p-values between groups of pre-CRT versus post-CRT and R versus NR was performed using Mann-Whitney U tests, p-values of <0.05 were considered significant. To account for multiple hypothesis testing, a Benjamini-Hochberg FDR of 0.1 was used to identify highly significant associations.

Immunohistochemistry

Details of the 6 antibodies (PD1, PD-L1, PD-L2, CTLA4, CD4, CD8), host species, clone, and dilatation are given in Supplemental Table 1. Immunohistochemistry (IHC) was performed automatically using a Benchmark XT/Discovery ULTRA Staining Module (Ventana Medical Systems, Inc., Tucson, AZ) using established protocols (42). In brief, protocols consisted of pretreatment with CC1 (pH 8.0), incubation with primary antibodies, and detection using a DAB-system (catalog No. 760-500, Ventana Medical Systems, Inc) including ultraview inhibitor, horseradish peroxidase, multimer chromogen, H2O2, and copper. In brief, sections were washed for 5 minutes (xylene x3, 100% ethanol x2, 95% ethanol x1, 70% ethanol x1, and PBS x1). Staining properties and specificity have been determined previously (Supplemental Table 1, (37,43–47)), which we additionally ascertained using negative and positive controls (Tonsil).

Microscopy and Quantification

For light microscopy, we captured images using an Olympus DP27 camera attached to an Olympus BX40 light microscope (Olympus America, Center Valley, PA). All markers were evaluated on tumor and non-tumor compartments and scored as positive vs. negative using established cut-offs (48–50). For CD4 and CD8 we additionally captured 4 images (high power field, 400x) and applied established image quantification tools. Briefly, segmentation of cells was achieved using threshold filters in combination with circularity and size cutoffs using “cell counter” and “analyze particle” plug-ins in Image J software (NIH, Bethesda, MD) (42). For statistical analysis of CD4 and CD8 staining of immune infiltrates, we took the average and median of four independent regions of interest. Differences in CD4 and CD8 T cell infiltrates between pre-/post-CRT samples were calculated using a t-test of changes with a null hypothesis of a difference of 0. $p<0.05$ was considered to be statistically significant. Correlations and associated p values between groups of pre-CRT versus post-

CRT, R versus NR, and KP genotype versus no KP genotype were performed using Mann-Whitney U tests, p-values of <0.05 were considered significant.

Outcome analysis

We analyzed the association between R versus NR and *KRAS/TP53* mutation genotype versus no *KRAS/TP53* mutation genotype with progression-free survival using the Kaplan-Meier method. All statistical tests were performed using R version 3.5.2 and Prism 8 software (GraphPad, La Jolla, CA, USA).

Data availability

All BAMS for the matched pre and post-treatment tumors will be deposited in dbGAP (phs001829.v1.p1).

RESULTS

Chemoradiation does not increase TMB or neoantigen load

We assembled a cohort of 17 patients with locally advanced rectal carcinoma, of whom 9 were characterized pathologically as responders (R) and 8 as nonresponders (NR) following neoadjuvant CRT (Methods). Tumor genotype was unknown at the time of case identification. These patients had sufficient pre-CRT biopsy tissue and post-CRT surgical resection tissue available for multiple analytical pipelines including deep whole exome sequencing (Figure 1a). Demographic, treatment, and tumor characteristics are summarized in Supplementary Tables 2 and 3. All tumors demonstrated microsatellite stability. Median follow-up of the cohort was 47.1 months (range, 5.8-90.6). There were no local tumor failures. Overall, NR status was associated with reduced progression-free survival (PFS) compared to R with 5-year PFS 44% versus 100%, respectively (log-rank p=0.02) (Figure 1b). Median PFS for NR and R was 24.8 months and not reached, respectively.

No statistically significant change in TMB before and after exposure to CRT was observed in our cohort (p=0.40, Figure 1c). A similar analysis of predicted neoantigen burden between pre- and post-CRT tumors also demonstrated no statistically significant change (p=0.12, Figure 1d). Neither pre- nor post-CRT neoantigen load were associated with treatment response (p=0.81, Supplemental Figure 1 and p=0.42, Supplemental Figure 2, respectively). We also found no difference in indel loads between pre- and post-treatment samples (p=0.20, Supplemental Figure 3). As has been previously demonstrated (51–54), the most frequently mutated genes pre- and post-CRT included *KRAS*, *TP53,* and *APC* (Figure 1e). Thus, global somatic mutations were not impacted by exposure to CRT in this cohort.

Presence of *KRAS* and *TP53* co-mutation predicts resistance to chemoradiation

In evaluating differences in specific somatic mutations between R versus NR cases, we observed that NR tumors were enriched for concurrent *KRAS* and *TP53* mutations (KP genotype) in contrast to R tumors (Fisher's exact p=0.05, Figure 2a–b), as has been previously described (55–57). Notably, one pre-CRT *KRAS*-mutated tumor harbored a *TP53* mutation post-CRT that was not detected in the pre-treatment tumor despite sufficient power to detect a mutation; this patient was also a NR (Figure 2c, Supplemental Figures 4–5),

suggesting emergence of a radioresistant subclone. Given its association with NR, we next investigated the association between KP genotype and PFS. Patients with the KP genotype experienced reduced 5-year PFS (38%) compared to those without (90%, log-rank p=0.04, Figure 2d).

Immune microenvironmental properties in rectal cancers treated with chemoradiation

To complement our investigation of tumor-intrinsic genomic properties discriminating response to CRT, we examined how transcriptional programs in the tumor or microenvironment were impacted by exposure to these therapies. Among the responders, there were 14 unique transcriptional programs significantly enriched in the pre-CRT samples and 1 unique transcriptional program significantly enriched in the post-CRT samples, with interferon alpha response genes enriched in both pre-/post-CRT samples (FWER p=0.00, Figure 3a). Among the NR, there were no unique significantly enriched transcriptional programs in the pre-CRT samples and there were 5 unique transcriptional programs significantly enriched in the post-CRT samples, with the angiogenesis and epithelial-mesenchymal transition (EMT) transcriptional programs enriched among both pre- and post-CRT samples (FWER p=0.00, Figure 3a).

Given the immune-related transcriptional programs enriched pre-/post-CRT, we next examined immune cell infiltrates inferred from bulk transcriptome data (Methods). Total immune infiltrate levels were significantly higher in post-CRT specimens relative to their pre-CRT counterparts (p=0.04, Figure 3b). Overall, we observed significantly more naïve B cells (p=0.044), CD8 T cells (p=0.002), monocytes (p=0.01), M2 macrophages (p=0.002), and resting mast cells (p=0.0007) in the post-CRT tumor specimens. In contrast, there were significantly more memory B cells (p=0.04) and activated mast cells (p=0.006) in the pre-CRT tumor specimens (Supplemental Figure 6).

Interestingly, when limiting the analysis to NR pre-/post-CRT, we observed significantly more M2 macrophages (p=0.005, FDR q=0.1) in the post-CRT tumor specimens, as well as naïve B cells (p=0.03), monocytes (p=0.03), and resting mast cells (p=0.03), with significantly more activated mast cells in the pre-CRT specimens (p=0.04) (Figure 3c).

To complement bulk transcriptome analysis, we also evaluated immune infiltrate using immunohistochemistry for CD4 and CD8 T cells (Supplemental Table 4). The number of CD8 T cells trended toward a global increase between pre-CRT and post-CRT samples (p=0.47, Supplemental Figure 7). In the pre-CRT samples, there were more CD8 T cells in R compared to NR (p=0.14, Figure 4a) and complete responders (CR) samples had significantly more CD8 immune infiltration compared to NR (p=0.04, Figure 4a–b, Supplemental Figures 8–9).

Globally, CD4 infiltrate decreased between pre- and post-CRT, but this trend was not statistically significant (p=0.89, Supplemental Figure 10). Similar to CD8 T cells, NR trended toward having less CD4 immune infiltration compared to R (p=0.32, Figure 4c). When further breaking down response into CR versus partial responders (PR), CR appeared to have more CD4 immune infiltrate compared to NR (p=0.37, Figure 4c–d, Supplemental Figures 11–12). In summary, while IHC demonstrated significant differences in T cell

infiltrate pre-CRT between R versus NR, clear shifts in immune infiltrate composition were observed after CRT in NR patients based on bulk transcriptome analysis.

DISCUSSION

To our knowledge, this is the first study to evaluate both genomic and microenvironmental changes at a primary rectal cancer tumor site exposed to preoperative CRT. Our data provide an opportunity to understand treatment-associated genomic changes between pre- and post-CRT specimens directly in patients. Tumor evolution has been previously studied primarily in the context of systemic cancer therapeutics in solid tumors (23,36,58–61), while most RT-based studies have examined candidate germline features or leveraged microarray data (11,12,62–75). Here we performed integrative comprehensive molecular characterization to dissect tumor and immune properties that track with CRT resistance.

Tumor mutation burden has been extensively studied and is suggested to be a marker of tumor-responsiveness to immune checkpoint blockade (18,19). It has been hypothesized that radiation may be able to increase TMB through its DNA-damaging mechanisms. Our data did not demonstrate an increase in overall mutational or neoantigen load after exposure to CRT. This finding is consistent with other pre- and post-matched tumor evolutionary assessments in the context of systemic therapy, particularly with cisplatin-based chemotherapy (23). Our data support the notion that chemotherapy or radiation are generally insufficient to prime the immune system by creating appropriate mutations or neoantigens (76,77).

While global genomic tumor properties were not clearly different between response groups, NR were more likely to harbor co-*KRAS/TP53* mutations compared to R. The KP genotype has been previously suggested to be associated with radioresistance but the underlying mechanisms are poorly understood (55–57). Our observations in KP/NR cases suggest a previously unrecognized mechanism of immune suppression (Figure 3). We demonstrated that NR were more likely to express a M2 macrophage phenotype as well as enrichment for an EMT transcriptional program in the post-CRT specimens. The M2 phenotype is known to be anti-inflammatory, pro-angiogenic, and metastasis-promoting (78–80), while EMT plays a role in cancer metastasis and treatment resistance (81–85). Thus, KP/NR status may be associated with local immune escape during or after CRT. Of note, in our cohort without local recurrences, we found that NR/KP was associated with metastatic progression. Taken together, this suggests that KP/NR-associated local immune escape leads to distant metastatic disease and reduced PFS (Figure 1b, 2d). Thus, these tumors may benefit from novel neoadjuvant treatment approaches to reduce the risk of immune escape and metastatic seeding.

There are several limitations to this study. Small patient numbers make additional in-depth analyses and conclusions difficult, hence our findings need validation in larger, independent cohorts in diverse clinical settings. Many of our associations may be dependent on one another, as we do not have enough events to appropriately determine whether *KRAS/TP53* genotype or pCR rate is more predictive of PFS through a multivariable regression. We rely on pCR as a biomarker of response, which has been called into question after preoperative

CRT for rectal cancer (86) as pCR can vary and may be a function of time between end of CRT and surgical resection, although it has been used as a robust endpoint when evaluating novel systemic agents in other solid tumors (4). Some of our findings may be attributable to samples having higher or lower initial tumor burden; to overcome this issue, we performed purity/ploidy corrected molecular analysis through the ABSOLUTE algorithm (35) to account for differences in stromally admixed tumor specimens. We did not evaluate the impact of short-course preoperative radiotherapy nor other high-dose ablative radiotherapy schedules, which may elicit more mutagenesis and an immune response within the tumor microenvironment due to the higher dose per fraction during treatment (16,17,87,88). We also acknowledge that interpretation of in silico derived neoantigens from the mutations for each sample requires significant validation for improved interpretation. In addition, tumor spatial heterogeneity cannot be ruled out in this study as we do not have data from multiple areas of each tissue sample.

Overall, our study creates a path forward by leveraging molecular profiling for consideration of pre-operative CRT in patients with locally advanced tumors. This study also highlights the larger opportunity for additional investigations to elucidate novel mechanisms behind radioresistance across solid tumors.

Supplementary Material

Refer to Web version on PubMed Central for supplementary material.

Funding/Acknowledgements:

Damon Runyon Foundation (E.M. Van Allen)

NCI U01CA220714 (H. Willers)

This work was funded in part by NIH Grant No. R01 CA225655 (J.K. Lennerz) and the content is solely the responsibility of the authors and does not necessarily reflect the official views of the NIH.

Disclosure of potential conflicts of interest:

E.M.V.

Advisory/Consulting: Tango Therapeutics, Genome Medical, Invitae, Illumina, Foresite Capital, Dynamo

Research support: Novartis, Bristol Myers Squibb

Equity: Tango Therapeutics, Genome Medical, Syapse, Microsoft

Travel reimbursement: Roche/Genentech

Patents: Institutional patents filed on ERCC2 mutations and chemotherapy response, chromatin mutations and immunotherapy response, and methods for clinical interpretation

T.S.H.

Advisory/Consulting: Merck, EMD Serono

Research Support: Taiho, Mobetron, Astra-Zeneca, Bristol Myers Squibb, Ipsen

R.B.C.

Advisory/Consulting: Amgen, Array Biopharma, Astex Pharmaceuticals, Avidity Biosciences, Bristol Myers Squibb, Chugai, Fog Pharma, Genentech, LOXO, Merrimack, N-of-one, Novartis, nRichDx, Roche, Roivant, Shire, Spectrum Pharmaceuticals, Symphogen, Taiho, and Warp Drive Bio

Research Support: Asana, AstraZeneca, Sanofi

Equity: Avidity Biosciences, nRichDx

REFERENCES

1. Miller KD, Siegel RL, Lin CC, Mariotto AB, Kramer JL, Rowland JH, et al. Cancer treatment and survivorship statistics, 2016. CA Cancer J Clin 2016;66:271–89 [PubMed: 27253694]
2. Brown JM, Carlson DJ, Brenner DJ. The tumor radiobiology of SRS and SBRT: are more than the 5 Rs involved? Int J Radiat Oncol Biol Phys 2014;88:254–62 [PubMed: 24411596]
3. Kim NK, Baik SH, Seong JS, Kim H, Roh JK, Lee KY, et al. Oncologic outcomes after neoadjuvant chemoradiation followed by curative resection with tumor-specific mesorectal excision for fixed locally advanced rectal cancer: Impact of postirradiated pathologic downstaging on local recurrence and survival. Ann Surg 2006;244:1024–30 [PubMed: 17122629]
4. Das S, Lo AW. Re-inventing drug development: A case study of the I-SPY 2 breast cancer clinical trials program. Contemporary clinical trials 2017;62:168–74 [PubMed: 28899813]
5. Blum Murphy M, Xiao L, Patel VR, Maru DM, Correa AM, F GA, et al. Pathological complete response in patients with esophageal cancer after the trimodality approach: The association with baseline variables and survival-The University of Texas MD Anderson Cancer Center experience. Cancer 2017;123:4106–13 [PubMed: 28885712]
6. Hellmann MD, Chaft JE, William WN Jr., Rusch V, Pisters KM, Kalhor N, et al. Pathological response after neoadjuvant chemotherapy in resectable non-small-cell lung cancers: proposal for the use of major pathological response as a surrogate endpoint. The Lancet Oncology 2014;15:e42–50 [PubMed: 24384493]
7. Spring L, Greenup R, Niemierko A, Schapira L, Haddad S, Jimenez R, et al. Pathologic Complete Response After Neoadjuvant Chemotherapy and Long-Term Outcomes Among Young Women With Breast Cancer. Journal of the National Comprehensive Cancer Network : JNCCN 2017;15:1216–23 [PubMed: 28982747]
8. Roh MS, Colangelo LH, O'Connell MJ, Yothers G, Deutsch M, Allegra CJ, et al. Preoperative multimodality therapy improves disease-free survival in patients with carcinoma of the rectum: NSABP R-03. J Clin Oncol 2009;27:5124–30 [PubMed: 19770376]
9. Minsky BD, Cohen AM, Kemeny N, Enker WE, Kelsen DP, Reichman B, et al. Enhancement of radiation-induced downstaging of rectal cancer by fluorouracil and high-dose leucovorin chemotherapy. J Clin Oncol 1992;10:79–84 [PubMed: 1727928]
10. Mohiuddin M, Hayne M, Regine WF, Hanna N, Hagihara PF, McGrath P, et al. Prognostic significance of postchemoradiation stage following preoperative chemotherapy and radiation for advanced/recurrent rectal cancers. International Journal of Radiation Oncology*Biology*Physics 2000;48:1075–80
11. Kamran SC, Mouw KW. Applying Precision Oncology Principles in Radiation Oncology. JCO Precision Oncology 2018:1–23 [PubMed: 30949620]
12. Hall WA, Bergom C, Thompson RF, Baschnagel AM, Vijayakumar S, Willers H, et al. Precision Oncology and Genomically Guided Radiation Therapy: A Report From the American Society for Radiation Oncology/American Association of Physicists in Medicine/National Cancer Institute Precision Medicine Conference. Int J Radiat Oncol Biol Phys 2018;101:274–84 [PubMed: 28964588]
13. Bristow RG, Alexander B, Baumann M, Bratman SV, Brown JM, Camphausen K, et al. Combining precision radiotherapy with molecular targeting and immunomodulatory agents: a guideline by the American Society for Radiation Oncology. The Lancet Oncology 2018;19:e240–e51 [PubMed: 29726389]
14. Demaria S, Coleman CN, Formenti SC. Radiotherapy: Changing the Game in Immunotherapy. Trends in cancer 2016;2:286–94 [PubMed: 27774519]

15. Kirsch DG, Diehn M, Kesarwala AH, Maity A, Morgan MA, Schwarz JK, et al. The Future of Radiobiology. Journal of the National Cancer Institute 2018;110:329–40 [PubMed: 29126306]
16. Burnette B, Fu YX, Weichselbaum RR. The confluence of radiotherapy and immunotherapy. Frontiers in oncology 2012;2:143 [PubMed: 23087904]
17. Kwilas AR, Donahue RN, Bernstein MB, Hodge JW. In the field: exploiting the untapped potential of immunogenic modulation by radiation in combination with immunotherapy for the treatment of cancer. Frontiers in oncology 2012;2:104 [PubMed: 22973551]
18. Rizvi NA, Hellmann MD, Snyder A, Kvistborg P, Makarov V, Havel JJ, et al. Cancer immunology. Mutational landscape determines sensitivity to PD-1 blockade in non-small cell lung cancer. Science (New York, NY) 2015;348:124–8
19. Samstein RM, Lee CH, Shoushtari AN, Hellmann MD, Shen R, Janjigian YY, et al. Tumor mutational load predicts survival after immunotherapy across multiple cancer types. Nature genetics 2019
20. Sauer R, Becker H, Hohenberger W, Rodel C, Wittekind C, Fietkau R, et al. Preoperative versus postoperative chemoradiotherapy for rectal cancer. N Engl J Med 2004;351:1731–40 [PubMed: 15496622]
21. Andre T, Boni C, Mounedji-Boudiaf L, Navarro M, Tabernero J, Hickish T, et al. Oxaliplatin, fluorouracil, and leucovorin as adjuvant treatment for colon cancer. N Engl J Med 2004;350:2343–51 [PubMed: 15175436]
22. Van Allen EM, Mouw KW, Kim P, Iyer G, Wagle N, Al-Ahmadie H, et al. Somatic ERCC2 mutations correlate with cisplatin sensitivity in muscle-invasive urothelial carcinoma. Cancer discovery 2014;4:1140–53 [PubMed: 25096233]
23. Liu D, Abbosh P, Keliher D, Reardon B, Miao D, Mouw K, et al. Mutational patterns in chemotherapy resistant muscle-invasive bladder cancer. Nature communications 2017;8:2193
24. Firehose. Computer Program. 2016.
25. Cibulskis K, McKenna A, Fennell T, Banks E, DePristo M, Getz G. ContEst: estimating cross-contamination of human samples in next-generation sequencing data. Bioinformatics 2011;27:2601–2 [PubMed: 21803805]
26. Lawrence MS, Stojanov P, Mermel CH, Robinson JT, Garraway LA, Golub TR, et al. Discovery and saturation analysis of cancer genes across 21 tumour types. Nature 2014;505:495–501 [PubMed: 24390350]
27. Cibulskis K, Lawrence MS, Carter SL, Sivachenko A, Jaffe D, Sougnez C, et al. Sensitive detection of somatic point mutations in impure and heterogeneous cancer samples. Nat Biotechnol 2013;31:213–9 [PubMed: 23396013]
28. Saunders CT, Wong WS, Swamy S, Becq J, Murray LJ, Cheetham RK. Strelka: accurate somatic small-variant calling from sequenced tumor-normal sample pairs. Bioinformatics 2012;28:1811–7 [PubMed: 22581179]
29. Ramos AH, Lichtenstein L, Gupta M, Lawrence MS, Pugh TJ, Saksena G, et al. Oncotator: cancer variant annotation tool. Hum Mutat 2015;36:E2423–9 [PubMed: 25703262]
30. Robinson JT, Thorvaldsdottir H, Winckler W, Guttman M, Lander ES, Getz G, et al. Integrative genomics viewer. Nat Biotechnol 2011;29:24–6 [PubMed: 21221095]
31. Thorvaldsdottir H, Robinson JT, Mesirov JP. Integrative Genomics Viewer (IGV): high-performance genomics data visualization and exploration. Briefings in bioinformatics 2013;14:178–92 [PubMed: 22517427]
32. Le X, Antony R, Razavi P, Treacy DJ, Luo F, Ghandi M, et al. Systematic Functional Characterization of Resistance to PI3K Inhibition in Breast Cancer. Cancer discovery 2016;6:1134–47 [PubMed: 27604488]
33. Rooney MS, Shukla SA, Wu CJ, Getz G, Hacohen N. Molecular and genetic properties of tumors associated with local immune cytolytic activity. Cell 2015;160:48–61 [PubMed: 25594174]
34. Nielsen M, Lundegaard C, Blicher T, Lamberth K, Harndahl M, Justesen S, et al. NetMHCpan, a method for quantitative predictions of peptide binding to any HLA-A and -B locus protein of known sequence. PloS one 2007;2:e796 [PubMed: 17726526]
35. Carter SL, Cibulskis K, Helman E, McKenna A, Shen H, Zack T, et al. Absolute quantification of somatic DNA alterations in human cancer. Nat Biotechnol 2012;30:413–21 [PubMed: 22544022]

36. Brastianos PK, Carter SL, Santagata S, Cahill DP, Taylor-Weiner A, Jones RT, et al. Genomic Characterization of Brain Metastases Reveals Branched Evolution and Potential Therapeutic Targets. Cancer discovery 2015;5:1164–77 [PubMed: 26410082]
37. Rodrigues DN, Rescigno P, Liu D, Yuan W, Carreira S, Lambros MB, et al. Immunogenomic analyses associate immunological alterations with mismatch repair defects in prostate cancer. The Journal of clinical investigation 2018;128:5185
38. Johnson WE, Li C, Rabinovic A. Adjusting batch effects in microarray expression data using empirical Bayes methods. Biostatistics (Oxford, England) 2007;8:118–27
39. Chakraborty S, Datta S, Datta S. Surrogate variable analysis using partial least squares (SVA-PLS) in gene expression studies. Bioinformatics 2012;28:799–806 [PubMed: 22238271]
40. Subramanian A, Tamayo P, Mootha VK, Mukherjee S, Ebert BL, Gillette MA, et al. Gene set enrichment analysis: a knowledge-based approach for interpreting genome-wide expression profiles. Proceedings of the National Academy of Sciences of the United States of America 2005;102:15545–50 [PubMed: 16199517]
41. Newman AM, Liu CL, Green MR, Gentles AJ, Feng W, Xu Y, et al. Robust enumeration of cell subsets from tissue expression profiles. Nat Methods 2015;12:453–7 [PubMed: 25822800]
42. Lennerz JK, Kim SH, Oates EL, Huh WJ, Doherty JM, Tian X, et al. The transcription factor MIST1 is a novel human gastric chief cell marker whose expression is lost in metaplasia, dysplasia, and carcinoma. The American journal of pathology 2010;177:1514–33 [PubMed: 20709804]
43. Lehe C, Ghebeh H, Al-Sulaiman A, Al Qudaihi G, Al-Hussein K, Almohareb F, et al. The Wilms' tumor antigen is a novel target for human CD4+ regulatory T cells: implications for immunotherapy. Cancer research 2008;68:6350–9 [PubMed: 18676860]
44. Maruse Y, Kawano S, Jinno T, Matsubara R, Goto Y, Kaneko N, et al. Significant association of increased PD-L1 and PD-1 expression with nodal metastasis and a poor prognosis in oral squamous cell carcinoma. International journal of oral and maxillofacial surgery 2018;47:836–45 [PubMed: 29395669]
45. Pardoll DM. The blockade of immune checkpoints in cancer immunotherapy. Nature reviews Cancer 2012;12:252–64 [PubMed: 22437870]
46. Steele KE, Tan TH, Korn R, Dacosta K, Brown C, Kuziora M, et al. Measuring multiple parameters of CD8+ tumor-infiltrating lymphocytes in human cancers by image analysis. Journal for immunotherapy of cancer 2018;6:20 [PubMed: 29510739]
47. Zheng B, Ren T, Huang Y, Sun K, Wang S, Bao X, et al. PD-1 axis expression in musculoskeletal tumors and antitumor effect of nivolumab in osteosarcoma model of humanized mouse. Journal of hematology & oncology 2018;11:16 [PubMed: 29409495]
48. Anagnostou V, Smith KN, Forde PM, Niknafs N, Bhattacharya R, White J, et al. Evolution of Neoantigen Landscape during Immune Checkpoint Blockade in Non-Small Cell Lung Cancer. Cancer discovery 2017;7:264–76 [PubMed: 28031159]
49. Chen PL, Roh W, Reuben A, Cooper ZA, Spencer CN, Prieto PA, et al. Analysis of Immune Signatures in Longitudinal Tumor Samples Yields Insight into Biomarkers of Response and Mechanisms of Resistance to Immune Checkpoint Blockade. Cancer discovery 2016;6:827–37 [PubMed: 27301722]
50. Reuben A, Gittelman R, Gao J, Zhang J, Yusko EC, Wu CJ, et al. TCR Repertoire Intratumor Heterogeneity in Localized Lung Adenocarcinomas: An Association with Predicted Neoantigen Heterogeneity and Postsurgical Recurrence. Cancer discovery 2017;7:1088–97 [PubMed: 28733428]
51. Baker SJ, Preisinger AC, Jessup JM, Paraskeva C, Markowitz S, Willson JK, et al. p53 gene mutations occur in combination with 17p allelic deletions as late events in colorectal tumorigenesis. Cancer research 1990;50:7717–22 [PubMed: 2253215]
52. Soussi T The p53 tumor suppressor gene: from molecular biology to clinical investigation. Annals of the New York Academy of Sciences 2000;910:121–37; discussion 37-9 [PubMed: 10911910]
53. Takayama T, Ohi M, Hayashi T, Miyanishi K, Nobuoka A, Nakajima T, et al. Analysis of K-ras, APC, and beta-catenin in aberrant crypt foci in sporadic adenoma, cancer, and familial adenomatous polyposis. Gastroenterology 2001;121:599–611 [PubMed: 11522744]

54. Vogelstein B, Fearon ER, Hamilton SR, Kern SE, Preisinger AC, Leppert M, et al. Genetic alterations during colorectal-tumor development. N Engl J Med 1988;319:525–32 [PubMed: 2841597]
55. Hong TS, Wo JY, Borger DR, Yeap BY, McDonnell EI, Willers H, et al. Phase II Study of Proton-Based Stereotactic Body Radiation Therapy for Liver Metastases: Importance of Tumor Genotype. Journal of the National Cancer Institute 2017;109
56. Wang M, Han J, Marcar L, Black J, Liu Q, Li X, et al. Radiation Resistance in KRAS-Mutated Lung Cancer Is Enabled by Stem-like Properties Mediated by an Osteopontin-EGFR Pathway. Cancer research 2017;77:2018–28 [PubMed: 28202526]
57. Duldulao MP, Lee W, Nelson RA, Li W, Chen Z, Kim J, et al. Mutations in specific codons of the KRAS oncogene are associated with variable resistance to neoadjuvant chemoradiation therapy in patients with rectal adenocarcinoma. Ann Surg Oncol 2013;20:2166–71 [PubMed: 23456389]
58. Faltas BM, Prandi D, Tagawa ST, Molina AM, Nanus DM, Sternberg C, et al. Clonal evolution of chemotherapy-resistant urothelial carcinoma. Nature genetics 2016;48:1490–9 [PubMed: 27749842]
59. Gerlinger M, Rowan AJ, Horswell S, Math M, Larkin J, Endesfelder D, et al. Intratumor heterogeneity and branched evolution revealed by multiregion sequencing. N Engl J Med 2012;366:883–92 [PubMed: 22397650]
60. Johnson BE, Mazor T, Hong C, Barnes M, Aihara K, McLean CY, et al. Mutational analysis reveals the origin and therapy-driven evolution of recurrent glioma. Science (New York, NY) 2014;343:189–93
61. Patch AM, Christie EL, Etemadmoghadam D, Garsed DW, George J, Fereday S, et al. Whole-genome characterization of chemoresistant ovarian cancer. Nature 2015;521:489–94 [PubMed: 26017449]
62. Agostini M, Zangrando A, Pastrello C, D'Angelo E, Romano G, Giovannoni R, et al. A functional biological network centered on XRCC3: a new possible marker of chemoradiotherapy resistance in rectal cancer patients. Cancer Biol Ther 2015;16:1160–71 [PubMed: 26023803]
63. Kim IJ, Lim SB, Kang HC, Chang HJ, Ahn SA, Park HW, et al. Microarray gene expression profiling for predicting complete response to preoperative chemoradiotherapy in patients with advanced rectal cancer. Dis Colon Rectum 2007;50:1342–53 [PubMed: 17665260]
64. Rimkus C, Friederichs J, Boulesteix AL, Theisen J, Mages J, Becker K, et al. Microarray-based prediction of tumor response to neoadjuvant radiochemotherapy of patients with locally advanced rectal cancer. Clin Gastroenterol Hepatol 2008;6:53–61 [PubMed: 18166477]
65. Akiyoshi T, Kobunai T, Watanabe T. Predicting the response to preoperative radiation or chemoradiation by a microarray analysis of the gene expression profiles in rectal cancer. Surgery today 2012;42:713–9 [PubMed: 22706722]
66. Cecchin E, Agostini M, Pucciarelli S, De Paoli A, Canzonieri V, Sigon R, et al. Tumor response is predicted by patient genetic profile in rectal cancer patients treated with neo-adjuvant chemo-radiotherapy. The pharmacogenomics journal 2011;11:214–26 [PubMed: 20368715]
67. Chen Z, Liu Z, Li W, Qu K, Deng X, Varma MG, et al. Chromosomal copy number alterations are associated with tumor response to chemoradiation in locally advanced rectal cancer. Genes, chromosomes & cancer 2011;50:689–99 [PubMed: 21584903]
68. Gantt GA, Chen Y, Dejulius K, Mace AG, Barnholtz-Sloan J, Kalady MF. Gene expression profile is associated with chemoradiation resistance in rectal cancer. Colorectal disease : the official journal of the Association of Coloproctology of Great Britain and Ireland 2014;16:57–66 [PubMed: 24034224]
69. Grade M, Gaedcke J, Wangsa D, Varma S, Beckmann J, Liersch T, et al. Chromosomal copy number changes of locally advanced rectal cancers treated with preoperative chemoradiotherapy. Cancer genetics and cytogenetics 2009;193:19–28 [PubMed: 19602460]
70. Ho-Pun-Cheung A, Assenat E, Bascoul-Mollevi C, Bibeau F, Boissiere-Michot F, Thezenas S, et al. A large-scale candidate gene approach identifies SNPs in SOD2 and IL13 as predictive markers of response to preoperative chemoradiation in rectal cancer. The pharmacogenomics journal 2011;11:437–43 [PubMed: 20644561]

71. Hur H, Kang J, Kim NK, Min BS, Lee KY, Shin SJ, et al. Thymidylate synthase gene polymorphism affects the response to preoperative 5-fluorouracil chemoradiation therapy in patients with rectal cancer. Int J Radiat Oncol Biol Phys 2011;81:669–76 [PubMed: 20932673]
72. Kim JC, Ha YJ, Roh SA, Cho DH, Choi EY, Kim TW, et al. Novel single-nucleotide polymorphism markers predictive of pathologic response to preoperative chemoradiation therapy in rectal cancer patients. Int J Radiat Oncol Biol Phys 2013;86:350–7 [PubMed: 23490283]
73. Nishioka M, Shimada M, Kurita N, Iwata T, Morimoto S, Yoshikawa K, et al. Gene expression profile can predict pathological response to preoperative chemoradiotherapy in rectal cancer. Cancer genomics & proteomics 2011;8:87–92 [PubMed: 21471518]
74. Watanabe T, Kobunai T, Akiyoshi T, Matsuda K, Ishihara S, Nozawa K. Prediction of response to preoperative chemoradiotherapy in rectal cancer by using reverse transcriptase polymerase chain reaction analysis of four genes. Dis Colon Rectum 2014;57:23–31 [PubMed: 24316942]
75. Watanabe T, Komuro Y, Kiyomatsu T, Kanazawa T, Kazama Y, Tanaka J, et al. Prediction of sensitivity of rectal cancer cells in response to preoperative radiotherapy by DNA microarray analysis of gene expression profiles. Cancer research 2006;66:3370–4 [PubMed: 16585155]
76. Giordano FA, Veldwijk MR, Herskind C, Wenz F. Radiotherapy, tumor mutational burden, and immune checkpoint inhibitors: time to do the math. Strahlentherapie und Onkologie : Organ der Deutschen Rontgengesellschaft [et al.] 2018;194:873–5
77. Helleday T Making immunotherapy 'cold' tumours 'hot' by chemotherapy-induced mutations - a misconception. Annals of oncology : official journal of the European Society for Medical Oncology 2019
78. Hanada T, Nakagawa M, Emoto A, Nomura T, Nasu N, Nomura Y. Prognostic value of tumor-associated macrophage count in human bladder cancer. International journal of urology : official journal of the Japanese Urological Association 2000;7:263–9 [PubMed: 10910229]
79. Leek RD, Lewis CE, Whitehouse R, Greenall M, Clarke J, Harris AL. Association of macrophage infiltration with angiogenesis and prognosis in invasive breast carcinoma. Cancer research 1996;56:4625–9 [PubMed: 8840975]
80. Lin EY, Li JF, Gnatovskiy L, Deng Y, Zhu L, Grzesik DA, et al. Macrophages regulate the angiogenic switch in a mouse model of breast cancer. Cancer research 2006;66:11238–46 [PubMed: 17114237]
81. Hugo H, Ackland ML, Blick T, Lawrence MG, Clements JA, Williams ED, et al. Epithelial--mesenchymal and mesenchymal--epithelial transitions in carcinoma progression. Journal of cellular physiology 2007;213:374–83 [PubMed: 17680632]
82. Theys J, Jutten B, Habets R, Paesmans K, Groot AJ, Lambin P, et al. E-Cadherin loss associated with EMT promotes radioresistance in human tumor cells. Radiotherapy and oncology : journal of the European Society for Therapeutic Radiology and Oncology 2011;99:392–7 [PubMed: 21680037]
83. Valastyan S, Weinberg RA. Tumor metastasis: molecular insights and evolving paradigms. Cell 2011;147:275–92 [PubMed: 22000009]
84. Zhang H, Luo H, Jiang Z, Yue J, Hou Q, Xie R, et al. Fractionated irradiation-induced EMT-like phenotype conferred radioresistance in esophageal squamous cell carcinoma. Journal of radiation research 2016;57:370–80 [PubMed: 27125498]
85. Zhou P, Li B, Liu F, Zhang M, Wang Q, Liu Y, et al. The epithelial to mesenchymal transition (EMT) and cancer stem cells: implication for treatment resistance in pancreatic cancer. Molecular cancer 2017;16:52 [PubMed: 28245823]
86. Rose BS, Winer EP, Mamon HJ. Perils of the Pathologic Complete Response. J Clin Oncol 2016;34:3959–62 [PubMed: 27551115]
87. Formenti SC, Rudqvist NP, Golden E, Cooper B, Wennerberg E, Lhuillier C, et al. Radiotherapy induces responses of lung cancer to CTLA-4 blockade. Nature medicine 2018;24:1845–51
88. van Gijn W, Marijnen CA, Nagtegaal ID, Kranenbarg EM, Putter H, Wiggers T, et al. Preoperative radiotherapy combined with total mesorectal excision for resectable rectal cancer: 12-year follow-up of the multicentre, randomised controlled TME trial. The Lancet Oncology 2011;12:575–82 [PubMed: 21596621]

SIGNIFICANCE/TRANSLATIONAL RELEVANCE

Integrated tumor profiling of patient-matched rectal adenocarcinomas before and after neoadjuvant chemo/radiation therapy reveals insights into tumor evolution and treatment resistance mechanisms. The inability of neoadjuvant therapy to enhance tumor mutational burden coupled with poor response and local immune escape, particularly in *KRAS/TP53*-mutated tumors, warrant novel treatment approaches.

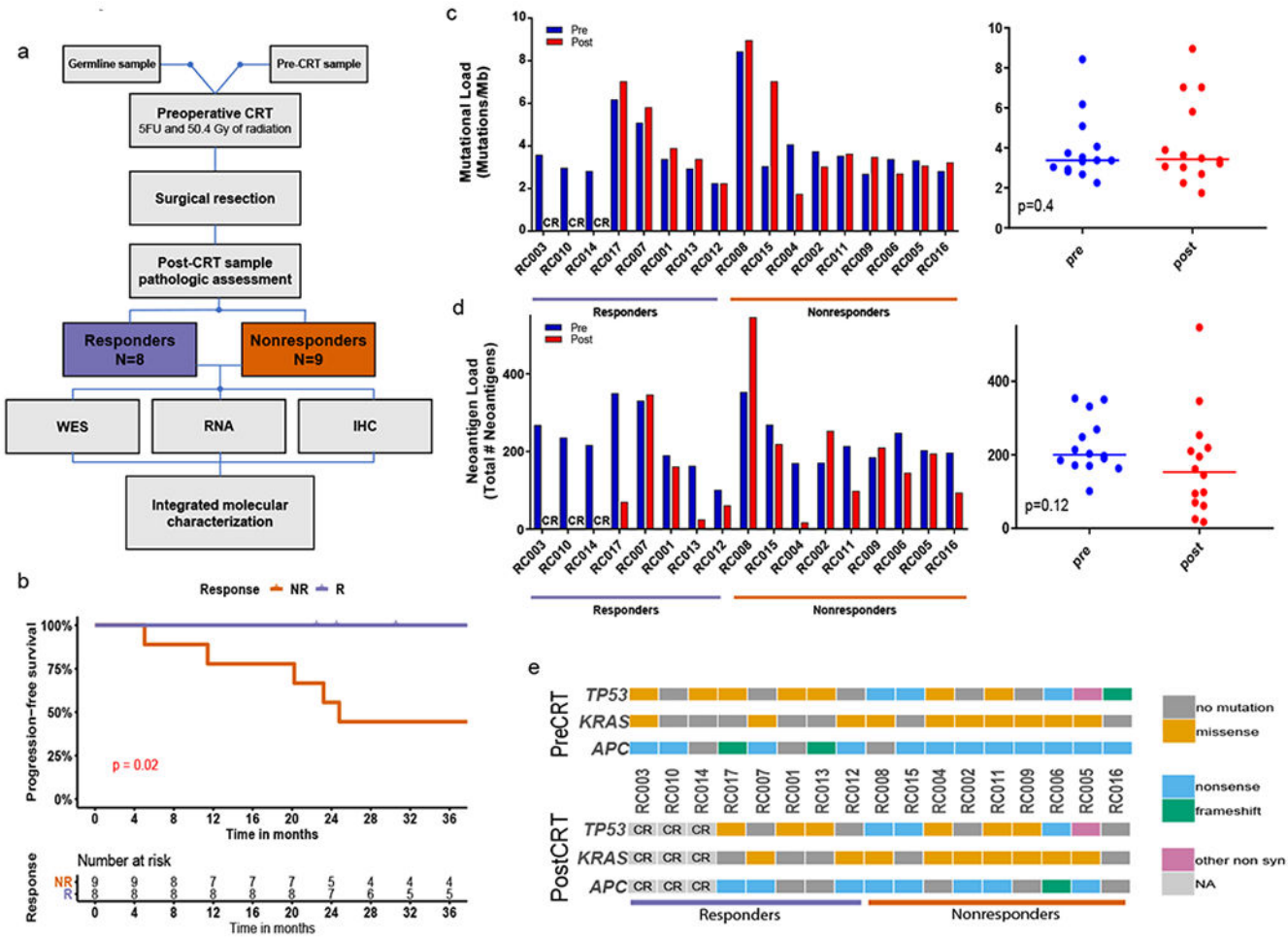

Figure 1. Integrated molecular characterization.

(A) Sample inclusion and analytical workflow. (B) Progression-free survival by response. NR predicted poorer PFS compared to R with 5-year PFS of 44% versus 100% (log-rank p=0.02). (C) Mutational burden in cohort (paired t-test, p=0.4). Patients are ordered by response group (responders, nonresponders), with tumor mutation burden in decreasing order within each response category. (D) Neoantigen load in cohort (paired t-test, p=0.12). (E) Mutations in the cohort. Shown are the genes that were most commonly mutated as assessed by MutSig2CV analysis. CRT, chemoradiation; WES, whole exome sequencing; RNA, RNA-sequencing; IHC, immunohistochemistry; CR, complete pathological response

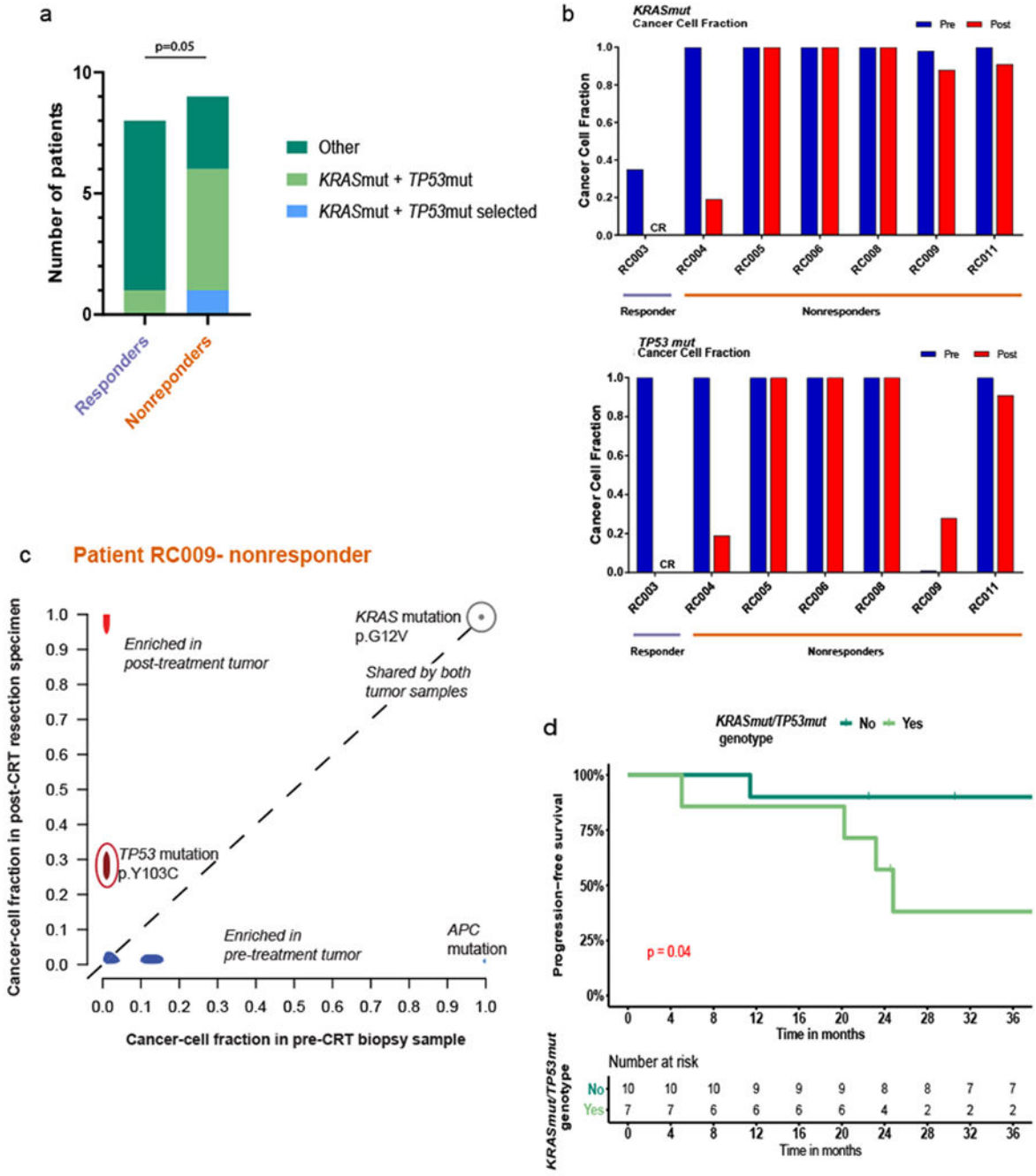

Figure 2. Co-mutation of *KRAS* and *TP53* predicts resistance to chemoradiation.

(A) NR tumors were enriched for concurrent mutations in *KRAS* and *TP53* genes compared to R (p=0.05, Fisher's exact test). (B) Cancer cell fraction pre-/post-CRT for the *KRAS* and *TP53* genes among the one R and six NR samples respectively. (C) Cancer cell fraction cluster plot for RC009 demonstrates the *TP53* mutation in the post-treatment clones. (D) Patients harboring the co-KP genotype had poorer 5-year PFS (38%, log-rank p=0.04). CR, complete pathological response

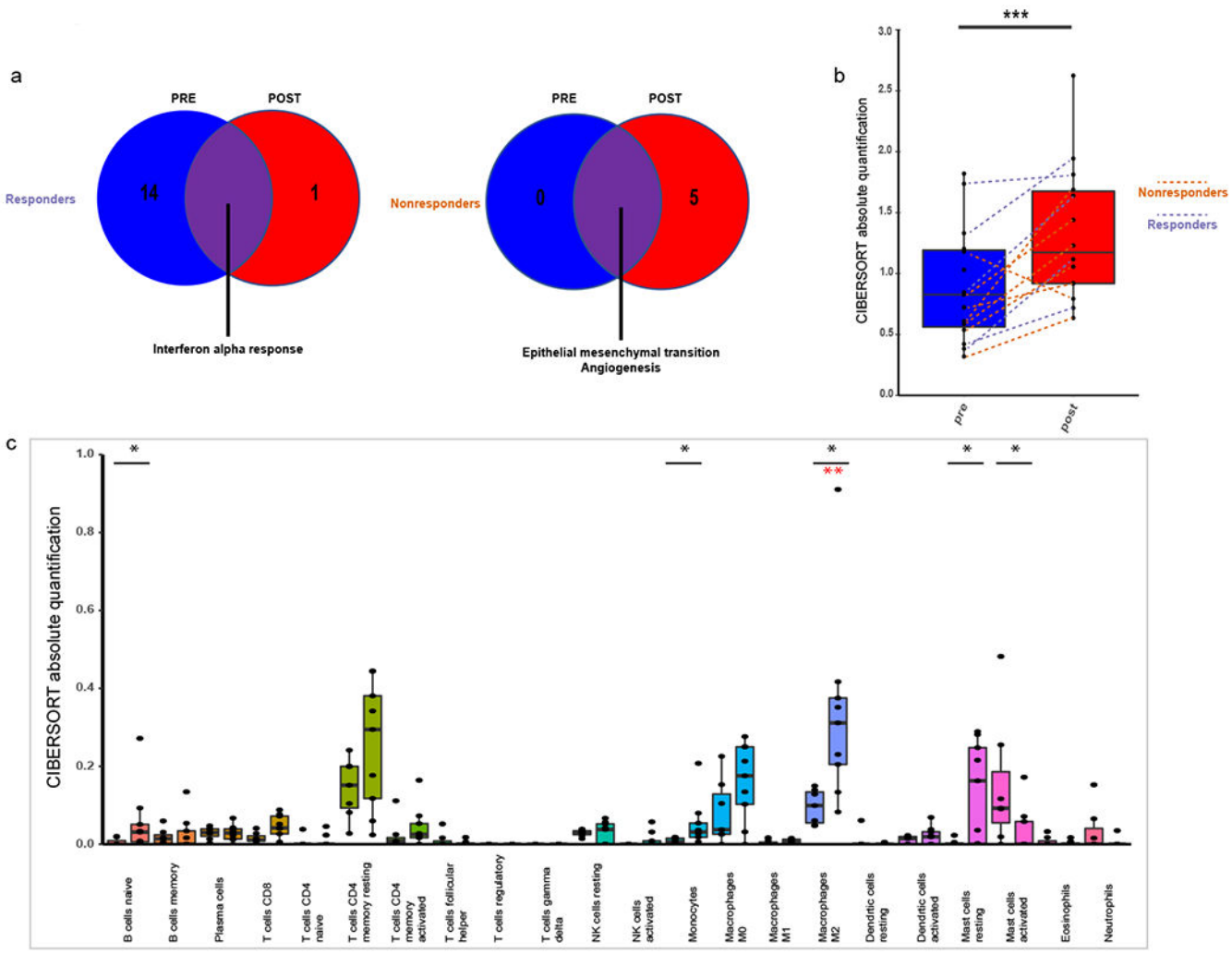

Figure 3. Transcriptome and gene expression profiling identifies unique mechanisms behind radiation resistance among pathologic nonresponders.

(A) Gene set enrichment analysis demonstrated interferon alpha response genes enriched in both pre-/post-CRT samples in the R (FWER p=0.00), while angiogenesis and epithelial-mesenchymal transition genes were enriched in both pre-/post-CRT samples in the NR (FWER p=0.00). (B) The y-axis is an absolute quantification. Dotted lines represent individual paired patients (R vs. NR). Immune cell infiltrate significantly increased between pre-/post-CRT samples (t-test, p=0.04). (C) The y-axis is an absolute quantification, x-axis denotes immune cell subset populations with pre/post next to each other for each individual subset. Increased M2 macrophages were observed in post-CRT specimens amongst NR (Mann-Whitney U p=0.005, Benjamini-Hochberg FDR q=0.1), along with increased naïve B cells (Mann-Whitney U, p=0.03), monocytes (Mann-Whitney U, p=0.03), and resting mast cells (Mann-Whitney U, p=0.03). *** denotes significance per t-test; * denotes significance per Mann-Whitney U; ** denotes significance per Benjamini-Hochberg FDR

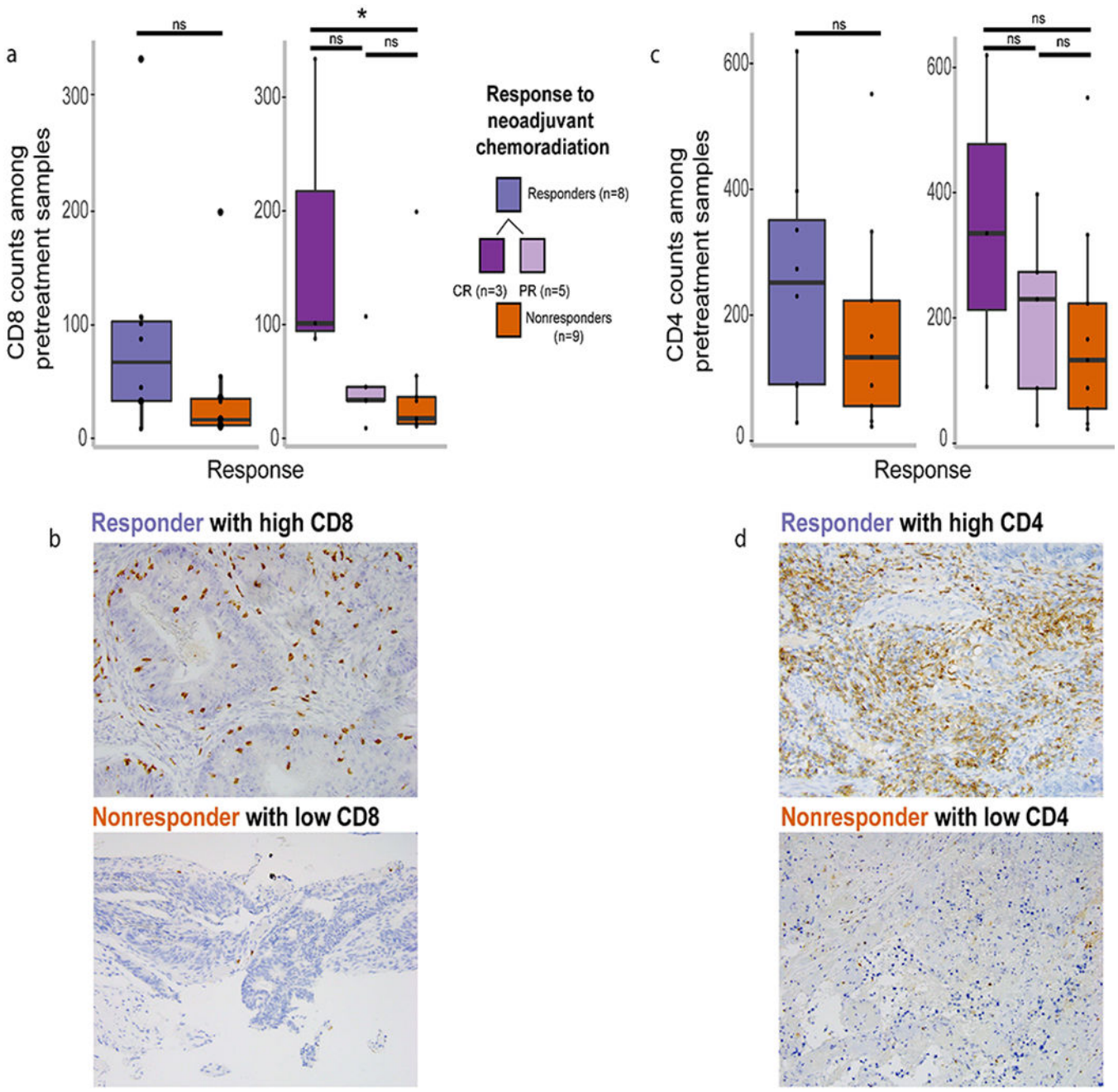

Figure 4. Immune infiltrate analysis by immunohistochemistry demonstrates shifts in immune cell composition after chemoradiation.

(A) Among the pre-CRT samples, there were more CD8 cells among R compared to NR, and CR samples had significantly more CD8 cells compared to NR (Mann-Whitney U, p=0.04). (B) Representative images of a R with high CD8 infiltrate and NR with low CD8 infiltrate in pre-CRT specimens. (C) Among the pre-CRT samples, CR had increased CD4 immune infiltrate compared to NR (Mann-Whitney U, p=0.37). (D) Representative images of a R with high CD4 infiltrate and NR with low CD4 infiltrate in pre-CRT specimens. CR, complete pathological response; PR, partial pathological response; *significant p-value; ns,

non-significant; Each individual dot represents the average of 4 independent regions of interest per patient.